

Classification of COVID-19 Cases from X-Ray Images Based on a Modified VGG-16 Model



Omar Sedqi Kareem^{1,2*}, Ahmed Khorsheed Al-Sulaifanie¹

¹ Department of Electrical and Computer Engineering, College of Engineering, University of Duhok, Duhok 42001, Iraq

² Department of Public Health, College of Health and Medical Techniques - Shekhan, Duhok Polytechnic University, Duhok 42001, Iraq

Corresponding Author Email: omar.kareem@dpu.edu.krd

<https://doi.org/10.18280/ts.390126>

ABSTRACT

Received: 14 December 2021

Accepted: 12 February 2022

Keywords:

Convolutional Neural Network, COVID-19, deep learning, VGG-16, computer-aided diagnosis, transfer learning, X-ray images, artificial neural network

COVID-19 is considered one of the most deadly pandemics by the World Health Organization and has claimed the lives of millions around the world. Mechanisms for early diagnosis and detection of this rapidly spreading disease are necessary to save lives. However, the increase in COVID-19 cases requires not relying on traditional means of detecting diseases due to these tests' limitations and high costs. One diagnostic technique for COVID-19 is X-rays and CT scans. For accurate and highly efficient diagnosis, computer-aided diagnosis is required. In this research, we suggest a convolutional neural network for chest x-ray images categorisation into two classes of infection: COVID-19 and normal. The suggested model uses an upgraded model based on the VGG-16 architecture that has been trained end-to-end on a dataset composed of X-ray images obtained from two different public data repositories, which include 1,320 and 1,578 cases in the COVID-19 and normal classes, respectively. This suggested model was trained and evaluated on the provided dataset and showed that our proposed model showed improved performance in the matter of overall accuracy, recall, precision, and F1-score at 99.54%, 99.5%, 99.5%, and 99.5%, respectively. The system's significance is supported because it has greater accuracy than other contemporary deep learning methods in the literature on COVID-19 identification.

1. INTRODUCTION

The viral family of coronaviruses causes illnesses and infections ranging from ordinary colds to SARS and MERS. A coronavirus called SARS-CoV-2 is responsible for the COVID-19 disease. An investigation by the World Health Organization (WHO) found that the COVID-19 virus, like SARS, leaves behind holes in the lungs that resemble a honeycomb. A case of COVID-19 initially emerged in December in Wuhan, Hubei, China [1]. The widespread diffusion of the coronavirus has isolated many individuals and hobbled numerous enterprises, thereby severely impairing quality of life. To avoid further harm, it is essential to control COVID-19 and to use the information to take preventative action [2]. However, demographic factors such as sex and age, as well as numerous urban circumstances like humidity and temperature, impact the transmission of this disease, including by enabling it to spread more effectively [3].

A major reason that it is difficult to identify and treat diseases is the absence of diagnostic instruments and the lack of available equipment for detection. Early diagnosis of COVID-19 will lower the number of COVID-19 victims, as well as those affected by other illnesses. The first step is to identify the coronavirus by recognising the symptoms and using unique indicators. Symptoms ranging from ordinary cold symptoms to fever, shortness of breath, cough, and severe respiratory difficulties might be the result of infection with one of the many coronaviruses [4]. The patient may experience a persistent cough for no obvious reason. SARS affects the respiratory system, but the coronavirus can spread to other

critical organs, such as the kidneys and liver. The extent to which people recover from the virus depends on their immune systems. WHO preventive guidelines for the virus include keeping a safe distance from others and practicing good hygiene [5].

COVID-19 can be detected using real-time polymerase chain reaction (RT-PCR). However, these results take time to verify and are costly. Antibodies that are created as a result of combating the virus can be found in the blood of infected persons. For most people, however, the antibodies do not form until 2 weeks after contracting the virus, making early diagnosis impossible with this test [4]. Medical image processing can address this challenge by improving health care for those who are co-infected with the COVID-19 virus. The medical imaging field relies heavily on X-rays and computed tomography (CT) scans, and several studies have utilized these to create models that can assist radiologists in anticipating illness [6]. Figure 1 shows a negative example with a regular chest X-ray and a positive example with COVID-19.

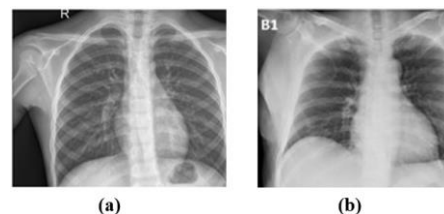


Figure 1. Samples of chest X-ray images (a) normal and (b) COVID-19

Deep Learning (DL) has opened a new path in the healthcare system. Deep neural networks have done their part to aid health care in a variety of ways, including the identification of diseases, such as chest illness, cancer cells and tumours, and even the study of genetic sequences [7, 8]. Machine learning has a variety of subcategories – among them, DL, which is employed to recognise and classify the features and objects seen in images. It has many applications, including helping with object recognition, and is also used in medical image classification [9]. Artificial intelligence systems have been used to mine, analyse and detect patterns in data for years, but the ability to do so more quickly and efficiently has only recently been discovered thanks to the widespread utilization of DL and machine learning algorithms [10, 11]. DL techniques frequently involve employing convolutional neural networks (CNNs) for bulk feature extraction. This method is commonly referred to as convolution. The layers can handle information that is not entirely linear [12]. The data are transformed into a higher and more abstract form at each layer. More information is learned as one travels further into the network. The inclusion of additional levels of information separation will make some elements vital for isolation and eliminate useless details. Usually, DL describes the use of large datasets and more sophisticated, deeper neural networks compared with classical machine learning, which relies on smaller datasets [13].

The main strengths and contributions of our proposed model are as follows:

- I. We develop a novel CNN model based on VGG-16 to discover and classify COVID-19-infected patients' X-ray chest images.
- II. The number of parameters in the VGG-16 model (more than 138 million) was reduced to about 25 million in our proposed model by minimising the number of filters at a higher level of the network.
- III. While most previous research used a limited number of COVID-19 patients, the current study employed a larger number.
- IV. Positive COVID-19 patients are accurately detected by the proposed model with 99% accuracy. The overall accuracy of the proposed model is 99.54%.

The paper is organised as follows: Section 2 discusses other research that has employed DL to diagnose COVID-19. Section 3 discusses our proposed network architecture and the DL approaches we used to analyse COVID-19 patients' X-ray images. In Section 4, we provide our system's experimental findings. In Section 5, we compare our models' performance to comparable systems and highlight the benefits of our method. Finally, we present the conclusion in Section 6.

2. RELATED WORKS

Since the start of the COVID-19 pandemic, researchers have attempted to use machine learning or deep neural networks to automatically detect COVID-19. In this subsection, recent research on COVID-19 detection and DL classifiers is presented.

Apostolopoulos and Mpesiana [10] looked at the most recent research investigating the accuracy of neural network designs in medical image analysis. The authors collected two various datasets of X-ray images available on public medical archives. The results showed that DL can extract important biomarkers associated with COVID-19, with the greatest

accuracy reaching 96.78%. Panwar et al. [13] suggested a DL model known as nCOVnet, which could be used to rapidly screen patients with COVID-19 using X-ray imaging. This fast screening method achieved 88.1% accuracy. An approach that automatically detects COVID-19 infection from chest X-ray images termed a deep CNN was proposed by Khan et al. [14]. The model is built on the Xception architecture and trained on an image dataset created by gathering data from databases of the X-ray images of two separate public sources. Overall, the suggested model obtained 99% accuracy in classifying the binary data. Bharati et al. [15] suggested a new hybrid DL architecture that combines VGG, data augmentation, and a spatial transformer network (STN) with a CNN. The new model was trained on a dataset of NIH chest X-ray images that was gathered from the Kaggle repository. Toraman et al. [16] presented Convolutional CapsNet, a new DL for detecting COVID-19 based on X-ray images. The suggested technique aims to ensure a quick and accurate diagnosis of binary-grade COVID-19 illnesses and obtain an accuracy of 97.24%. Shibly et al. [17] introduced a VGG-16 Faster region with a Faster R-CNN frame, using an open-source dataset to identify patients with COVID-19 based on X-ray images. The accuracy of this method is 97.36%. Abraham and Nair [18] focused on evaluating the capability of a multi-CNN system to automatically identify COVID-19 in X-ray images. A multi-CNN was used with a CFS and Bayes net classifier to perform COVID-19 prediction. The technique has 97.44% accuracy. Varela-Santos and Melin [19] presented an early experiment utilizing image texture feature descriptors, a feedforward network, and a CNN on freshly built datasets using COVID-19 pictures, laying the foundation for future development of a system capable of automatically identifying COVID-19 in chest X-rays and CT images of the lungs. A histogram equalization method and a bilateral low-pass filter were used in the study of Heidari et al. [20] to create a pseudo-colour picture for detecting COVID-19 infection and pneumonia. Pandit et al. [21] suggested a model that used chest radiographs because the rapidity and inexpensive cost of these imaging modalities make them popular for clinical diagnosis. The model investigated the VGG-16 model's ability for categorisation. This study employed transfer learning with fine-tuning to train the network on tiny chest radiographs. The trial demonstrated 96% accuracy in binary classification. Saha et al. [7] designed a detection system known as EMCNet to identify patients with COVID-19 in chest X-rays. The COVID-19 X-ray imaging model extracts detailed and complex information from infected individuals. Machine learning binary classifiers (decision tree, support vector machine, AdaBoost, and random forest) were created using the retrieved features for COVID-19 detection. The suggested model demonstrates higher accuracy of 98.91%. Sheykhivand et al. [22] offered a new approach to automated COVID-19 identification using deep neural networks. Their architecture used generative adversarial networks combined with transfer learning to diagnose COVID-19 without the need for feature extraction. The procedure was able to successfully separate COVID-19 from the healthy group with 99% accuracy. Adedigba et al. [23] proposed a computerized approach for optimizing hyper-parameters. They explored how learning rates may be individually tuned to each layer of the network to fine-tune the parameters. Their model was able to execute at a high level and generalise well, with 96.83% accuracy. The COV-SNET model presented by Hertel and Benlamri [24] was trained on over 100,000 X-ray images. Two models were

developed to diagnose COVID-19 using COV-SNET. These DL models were quite robust, reaching 95% sensitivity rates for the three-class and two-class models. The research of Dilshad et al. [25] sought to establish a transfer learning model for early automated screening that offers the best accuracy and low false negatives along with low computational costs. They evaluated its performance using metrics to assist radiologists and further tested the model's performance in countries with low doctor-to-patient ratios, like India.

3. MATERIAL AND METHODOLOGY

An automated COVID-19 detection system was developed utilizing VGG16. Data were obtained from several sources. After they were gathered, the pictures were compressed. To avoid overfitting and enhance generalisation, the dataset was standardized. The data were separated into three groups: training, validation, and testing.

3.1 Dataset description

In the suggested method, datasets were obtained from several sources. First, the 576 X-ray images of COVID-19 available through the Kaggle repository, established by the research [26], include 1,583 negative images. This resource is devoted to X-ray pictures of patients with COVID-19, patients with pneumonia, and normal cases. The images were acquired from free sources and medical centres and are used for binary classification. We mixed these images with another dataset containing positive and negative COVID-19 images to increase the number of positive COVID-19 cases, thereby reaching 1,320 images [27]. The final dataset had a total of 2,898 images. The data were separated into three groups: 2,028 training images, 435 validation images, and 435 testing images. This division is illustrated in Table 1.

Table 1. Summary of dataset partition to three sets

Dataset	COVID-19	Normal	Total
Training	920	1108	2028
Testing	200	235	435
Validation	200	235	435
Total	1320	1578	2898

3.2 Deep transfer learning

A large amount of data is needed to attain accurate feature extraction and classification with DL models. Medical data analysis is important, but if a disease is at an early stage, like pneumonia, the dataset is limited [28]. CNN's typically

outguess in larger compared with smaller datasets [2]. Transfer learning is a prevalent deep learning strategy in which a model is redesigned and trained to solve a similar problem. Transfer learning enhances learning in a new problem by transferring previously learned knowledge. The weights in the layers were reused as a starting point for the training process and then adapted according to the current challenge. In CNN implementations where the amount of data collected is not significant, transfer learning may be helpful [29]. The transfer learning principle is visualised in Figure 2. This allows models pre-trained on large and challenging image datasets such as the ImageNet 1000-class classification competition to be used for applications with less amount dataset.

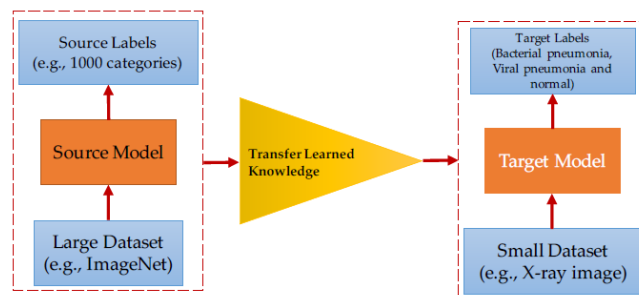


Figure 2. Diagram of transfer learning

Transfer learning has been successfully applied in various fields in engineering. Therefore, removing the requirement for a long training period and having a large dataset should be available when developing DL algorithms from scratch [30]. Many popular CNNs that have been pre-trained using DL, like AlexNet, VGG-16, Inception-v1, Inception-v3, ResNet-50, Inception-ResNet-V2, and ResNeXt-50, have been used for pneumonia detection.

3.3 CNN architecture of VGG-16

The researchers of the Visual Graphics Group at Oxford University designed this network, which is characterized by its pyramid-like structure. Its constituent layers consist of many convolutional layers followed by pooling layers that are combined by bundling layers to create a smaller layer shape [15]. Another benefit is offering excellent infrastructure for every mission, which allows them to set a benchmark. VGG-16 networks are utilised for a variety of applications, and pre-trained VGG networks are employed in even more contexts. The procedure is painstaking and time-consuming, and a significant amount of computational cost is required, as seen in Figure 3.

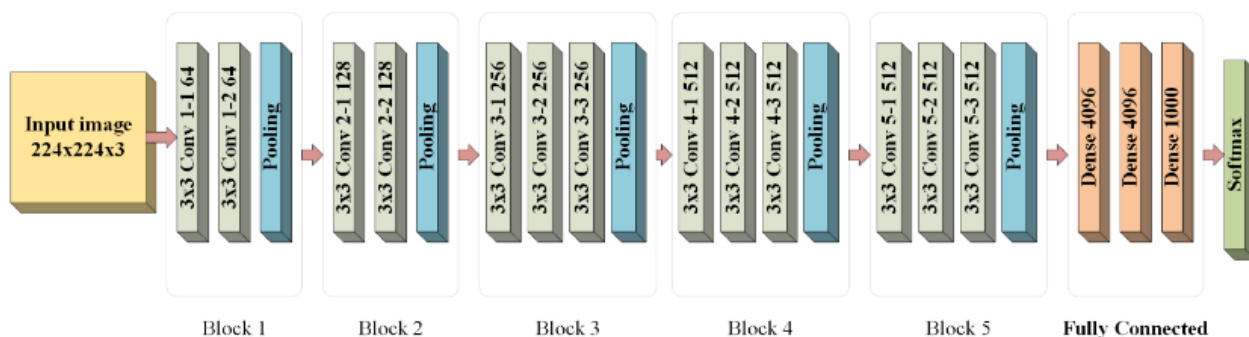


Figure 3. CNN model based on VGG16 architecture

The images fed to the VGG-16 model are $224 \times 224 \times 3$ pixels. The VGG-16 network contains 13 convolutional layers, five max-pooling layers, and three fully-connected layers arranged in six blocks, with 138 million trainable parameters in total. For the first five blocks of the VGG-16 model, all linked nodes in the front and low layers do not change weights. In addition, the fully connected block included three fully connected layers, with 4,096, 4,096, and 1,000 nodes, respectively. ReLU is employed as the activation function for these layers [20].

3.4 Proposed method architecture

This subsection describes the proposed model for automated COVID-19 classification. It is necessary to develop a technique for detecting patients with COVID-19 and thereby preventing infection with the virus that ensures the efficiency of detection while keeping the cost of RT-PCR detection as low as possible. We improved the VGG-16 network to extract features. The three-layer types included in VGG-16 are convolutional, max-pooling, and fully connected. To train the model, images (resized to 128×128) are input into the VGG-16 network. The number of blocks remains the same, but the modification occurs in the number of convolutional layers in each block (which becomes two), the number of kernel filters in each layer, the addition of batch normalisation, and the addition of dropout at the end of the block. Additionally, both the convolutional layer and the completely connected layer have activation layers and normalising layers: ReLU and a normalisation layer. To accelerate the convergence of the neural network and minimise the issue of “gradient explosion,” COVID-19 image batch processing is normalised. By utilising the suggested model, we increased the speed and accuracy of training and minimised the model’s dependency on the initial weights. The first step of classification is converting the feature extraction layer output into a one-dimensional data vector in a flattened layer. There are two layers of classification, each having 2,048 neurons, with a dropout layer between them. Dropout is a regularisation strategy that prevents complicated co-adaptations on training data, hence reducing overfitting in artificial neural networks. When all of the weights are learned together, it is normal for some of the relationships to be more predictive than others, as shown Eq. (1) [31]. This image classification is built using a dense layer with two neurons and the Softmax activation function. It identifies the chest diseases class as either COVID-19 or normal, as shown in Figure 4, with 25 million trainable parameters in total.

$$s_i(i) = \sum_{j=1}^n w_{ij} \delta_j I_j \quad (1)$$

Layer (type)	Output Shape	Param #
conv2d_1 (Conv2D)	(None, 128, 128, 32)	896
batch_normalization_1 (Batch Normalization)	(None, 128, 128, 32)	128
conv2d_2 (Conv2D)	(None, 128, 128, 32)	9248
batch_normalization_2 (Batch Normalization)	(None, 128, 128, 32)	128
max_pooling2d_1 (MaxPooling2D)	(None, 64, 64, 32)	0
dropout_1 (Dropout)	(None, 64, 64, 32)	0
conv2d_3 (Conv2D)	(None, 64, 64, 64)	18496
batch_normalization_3 (Batch Normalization)	(None, 64, 64, 64)	256
conv2d_4 (Conv2D)	(None, 64, 64, 64)	36928
batch_normalization_4 (Batch Normalization)	(None, 64, 64, 64)	256
max_pooling2d_2 (MaxPooling2D)	(None, 32, 32, 64)	0
dropout_2 (Dropout)	(None, 32, 32, 64)	0
conv2d_5 (Conv2D)	(None, 32, 32, 128)	73856
batch_normalization_5 (Batch Normalization)	(None, 32, 32, 128)	512
conv2d_6 (Conv2D)	(None, 32, 32, 128)	147584
batch_normalization_6 (Batch Normalization)	(None, 32, 32, 128)	512
max_pooling2d_3 (MaxPooling2D)	(None, 16, 16, 128)	0
dropout_3 (Dropout)	(None, 16, 16, 128)	0
conv2d_7 (Conv2D)	(None, 16, 16, 256)	295168
batch_normalization_7 (Batch Normalization)	(None, 16, 16, 256)	1024
conv2d_8 (Conv2D)	(None, 16, 16, 256)	590880
batch_normalization_8 (Batch Normalization)	(None, 16, 16, 256)	1024
max_pooling2d_4 (MaxPooling2D)	(None, 8, 8, 256)	0
dropout_4 (Dropout)	(None, 8, 8, 256)	0
conv2d_9 (Conv2D)	(None, 8, 8, 512)	1180160
batch_normalization_9 (Batch Normalization)	(None, 8, 8, 512)	2048
conv2d_10 (Conv2D)	(None, 8, 8, 512)	2359808
batch_normalization_10 (Batch Normalization)	(None, 8, 8, 512)	2048
max_pooling2d_5 (MaxPooling2D)	(None, 4, 4, 512)	0
dropout_5 (Dropout)	(None, 4, 4, 512)	0
flatten_1 (Flatten)	(None, 8192)	0
dense_1 (Dense)	(None, 2048)	16779264
dropout_6 (Dropout)	(None, 2048)	0
dense_2 (Dense)	(None, 2048)	4196352
dropout_7 (Dropout)	(None, 2048)	0
dense_3 (Dense)	(None, 2)	4098
Total params: 25,699,874		
Trainable params: 25,695,906		
Non-trainable params: 3,968		

Figure 5. Summary of the proposed model

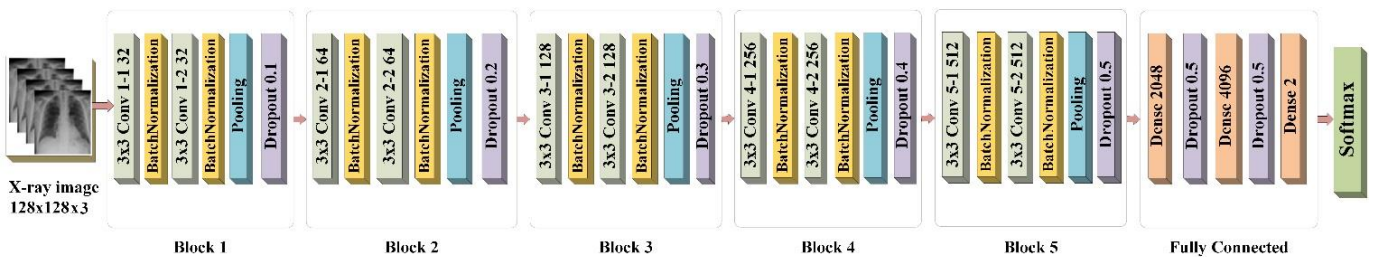


Figure 4. The architecture of the proposed model

Hyperparameters are crucial training parameters that affect the accuracy of a model. Selecting values for hyperparameters heavily influences a model's success. The most typical hyperparameters for DL models are learning rate, batch size, number of intervals, number of dense layers, and weights. For binary and multi-class classifications, categorical cross-entropy is utilised as a loss function. Each class is given a distinct number. Cross-entropy will compute a score that represents the average difference between the actual and predicted probability distributions if the data belongs into one of two classes. Computation of the average loss has been shown in Eq. (2) [32]. Table 2 describes our model's hyperparameters.

$$L = -\frac{1}{N} \sum_{i=1}^n (y_i \log(\hat{y}_i) + (1 - y_i) \log(1 - \hat{y}_i)) \quad (2)$$

Table 2. The proposed model's hyperparameters

Hyperparameters	Value
Learning rate	0.001
Batch size	16
Epochs	50
Optimiser	SGD
Momentum	0.95
Activation function	Softmax
Loss function	sparse categorical crossentropy

Furthermore, we built a completely new DL model from scratch utilising the five proposed layers, then trained it using the COVID-19 dataset. Binary classification is performed with the Softmax function. Figure 5 summaries the modifications made to the VGG-16 architecture model.

4. EXPERIMENTAL RESULTS

The proposed model was trained on a dataset composed of X-ray images. The measurement criteria parameters were considered to appraise the model's performance in diagnosing COVID-19 cases. The experiments were performed using a laptop core i7-5600U CPU 2.60GHz, NVidia GeForce 840M 2GB GPU, and RAM 16GB. The classification was performed by installing the anaconda python 3.7 as a software tool. A new environment has been installed with many libraries such as TensorFlow, Keras, CV2, Matplotlib, Pandas, and NumPy.

4.1 Performance metrics of classification

The performance of DL models was evaluated to determine the results of diagnosed COVID-19 cases in images by using different classification assessment tools, like accuracy, precision, sensitivity, specificity, and F1-score, which are defined as follows [33].

Accuracy: This metric is the most important for evaluating the DL classification.

$$Accuracy = \frac{(TP + TN)}{(TP + TN + FP + FN)} \quad (3)$$

Precision: It is a metric of accuracy, calculated by dividing correct positive predictions (identified as true positives) by the number of all positive predictions.

$$Precision = \frac{TP}{(TP + FP)} \quad (4)$$

Sensitivity (Recall): Perfection is measured, calculated by dividing the number of true positives by the number of actual positives.

$$Recall = \frac{TP}{(TP + FN)} \quad (5)$$

Specificity: It is calculated by dividing the number of true negatives by the total number of negatives in the data.

$$Specificity = \frac{TN}{(TN + FP)} \quad (6)$$

F1-score: It is a combination of the model's recall and precision that gives a better measure of the incorrectly classified cases.

$$F1 = \frac{2(precision * sensitivity)}{(precision + sensitivity)} \quad (7)$$

This helped patients with COVID-19 disease to be identified, along with the number of normal pictures identified as normal, the number of normal pictures wrongly identified, and the number of COVID-19 pictures falsely identified as normal [34].

4.2 Results evaluation and analysis

We used the confusion matrix to analyse the proposed model as well as plot training accuracy. Figure 6 illustrates the primary parameters for the confusion matrix: True Positive (TP), False Positive (FP), False Negative (FN), and True Negative (TN). The actual class values are listed in rows, while the predicted class values are represented in columns. This method has been commonly used to evaluate model success.

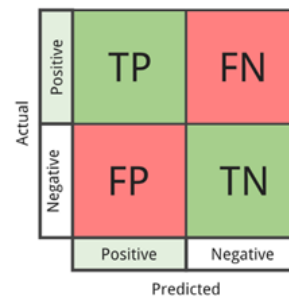


Figure 6. Confusion matrix

The suggested approach was trained for up to 50 epochs and 100 epochs using a dataset that was first partitioned into three parts: 75%, 15%, and 15% for training, testing, and validation, respectively. The accuracy of the training and validation results for 50 epochs is shown in Figure 7. A maximum training accuracy of 100% was reached, while the validation accuracy was 99.54%. The loss of training was 0.00032, while the loss of validation was 0.0287.

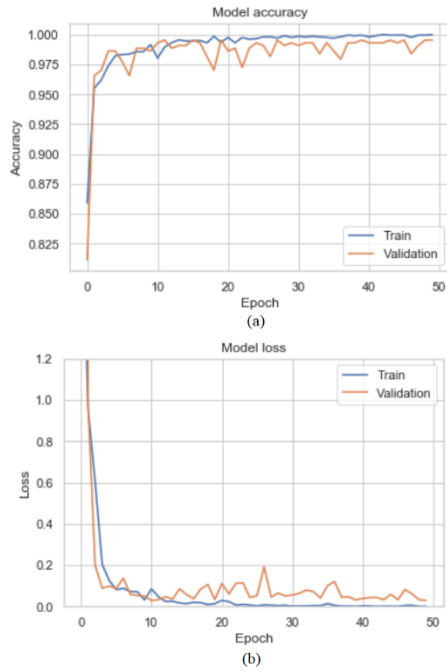


Figure 7. Performance analysis of accuracy and loss for training and validation of 50 epochs (a) Accuracy. (b) Loss

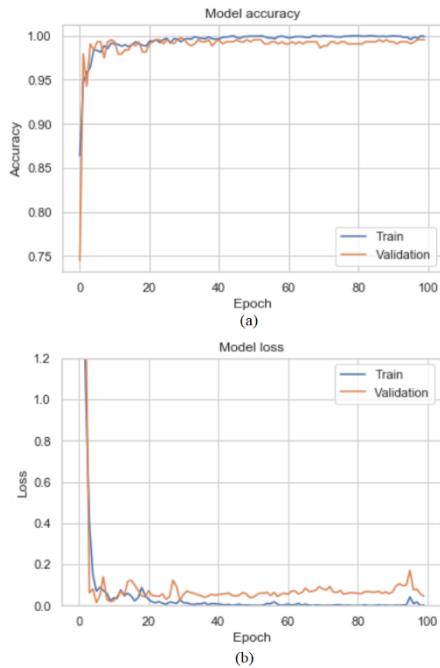


Figure 8. Performance analysis of accuracy and loss for training and validation of 100 epochs (a) Accuracy. (b) Loss

In addition, 100 epochs are shown in Figure 8. The model's maximum training accuracy reached is 100%, while the validation accuracy is 99.77%. These results suggest that our model learned effectively and was able to correctly categorise instances of persons with COVID-19 versus those without the

disease. The loss of training is 0.00032, while the loss of validation is 0.0142.

The confusion matrices shown in Figure 9 illustrate the achieved results of the proposed model for the 50 and 100 epoch values. For 50 epochs, the total number of images for the test was 235 for normal patients and 200 images for COVID-19 patients. The actual and anticipated instances were inserted in rows and columns, respectively, in the confusion matrices. Of our 200 COVID-19 patients, the model accurately recognised 198 and misdiagnosed only two as healthy. In addition, of the 235 normal instances, the model had 100% accuracy in determining which patients were normal. For 100 epochs, the model accurately recognised 197 of our 200 COVID-19 patients and misdiagnosed three as healthy. In addition, of the 235 normal instances, the model had 100% accuracy in determining which were normal.

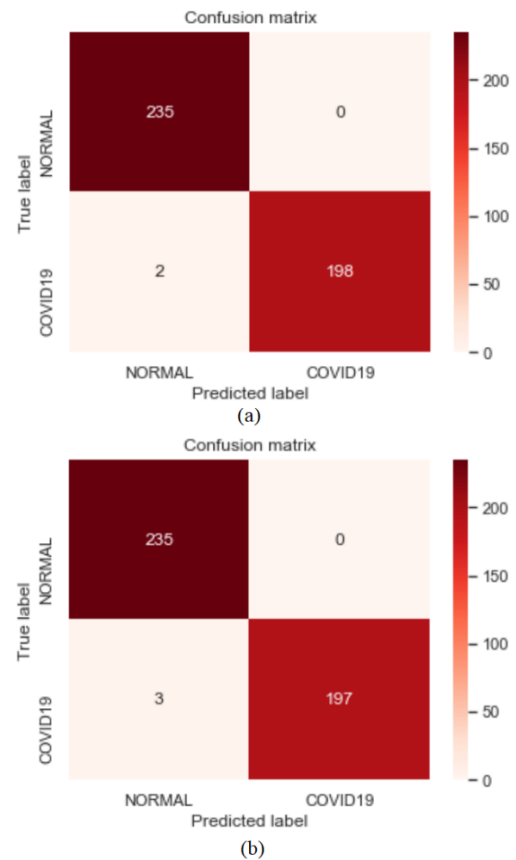


Figure 9. Confusion matrix representation for testing dataset (a) 50 epochs. (b) 100 epochs

The precision, recall, accuracy, specificity, and F1-score for each classifier (COVID-19 vs. normal) are presented in Table 3. The overall proposed model achieved 99.5% recall, 99.5% precision, 99.5% accuracy, and 99.5% F1-score for the binary class in training 50 epochs. In the second case (100 epochs), overall results indicated 98.74% precision, 100% recall, 99.31% accuracy, and 99% F1-score.

Table 3. Performance evaluation based on modified VGG-16 model

Epochs	Case classify	Evaluation metrics				Accuracy of proposed model %
		Recall%	Precision%	Specificity%	F1-score%	
50 epochs	COVID-19	99	100	99	99	99.54%
	Normal	100	99	100	100	
100 epochs	COVID-19	98	100	98.5	99	99.31%
	Normal	100	99	100	99	

5. DISCUSSION

Table 4. The comparison suggested model with other researches

Study	Dataset	Architecture	Performance measurement			
			Acc.	Sens.	Prec.	F1
Apostolopoulos and Mpesiana [10]	Two dataset 1427 and 1442 Covid-19 = (224&224) Pneumonia = (700&714) Normal = (504&504)	Transfer learning (VGG-19)	Binary = 98.75%	98.66%	-	-
Panwar et al. [13]	Cohen et al. Covid-19 = 192 Normal = 142 COVID-19 = 284 Pneumonia Bacterial = 330	nCOVnet	88.1%	-	-	-
Khan et al. [14]	Pneumonia Viral = 327 Normal = 310	CoroNet	Binary = 99%	99.3%	98.3%	98.5%
Toraman et al. [16]	Cohen et al. COVID-19 = 231 Pneumonia = 1050 Normal = 1050	CapsNet	Binary = 97.24%	97.42%	97.08%	97.24%
Shibly et al. [17]	X-ray images COVID-19 = 183 Normal = 13617	Faster R-CNN	97.36%	97.65%	99.28%	98.46%
Abraham and Nair [18]	Two dataset X-ray 950 and 78 Covid-19 = (453&71) Normal = (497&7) X-ray images 8474	CFS technique and Bayesnet classifier	Dataset1 = 91.2% Dataset2=97.36%	98.6%	98.6%	98.6%
Heidari et al. [20]	COVID-19 = 415 Pneumonia = 5179 Normal = 2880	VGG16	Binary = 98.1%	98.4%	-	-
Pandit et al. [21]	X-ray images COVID-19 = 224 Pneumonia = 700 Normal = 504	Transfer learning (VGG16)	Binary = 96%	92.64%	-	-
Saha et al. [7]	Cohen et al. COVID-19 = 2300 Normal = 2300	EMCNet	98.91%	97.82%	100%	98.89%
Sheykhivand et al. [22]	X-ray images COVID-19 = 371 Pneumonia Bacterial = 2778 Pneumonia Viral = 2840 Normal = 2923	GANs and Transfer learning and LSTM	Binary = 99%	100%	-	-
Hertel and Benlamri [24]	X-ray images COVID-19 = 358 Pneumonia = 5541 Normal = 8066	COV-SNET	Binary = 88.5%	95%	-	-
Fang and Wang [35]	CT scan image COVID-19 = 666 Normal = 794	CNN	97.3%	98%	97%	-
Dilshad et al. [25]	X-ray images COVID-19 = 447 Normal = 447	MobileNet	96.33%	93%	93%	-
Our proposed model	X-ray images COVID-19 = 1320 Normal = 1578	Modified VGG-16	99.54%	99.5%	99.5%	99.5%

We developed a new DL model based on VGG-16 to identify and classify COVID-19 infections based on X-ray images. This study differs from prior research in this field in numerous ways and makes several new intriguing observations. Initially, in the advanced levels of feature

extraction for the CNN model, the number of filters increased as with VGG-16. However, we reduced the number of layers from three to two in the last three blocks. A second consideration is that, since the CNN model has a significant number of parameters that must be trained and identified,

robust results require a large and diverse image dataset. Therefore, the number of parameters (more than 138 million in the VGG-16 model) was reduced to about 25 million in our proposed model. In addition, we trained the proposed model over 50 epochs and 100 epochs, and we obtained a better result in the first case, which reduces the time consumed in training the network (Table 4). Compared with prior research, our model's results are superior. A description of the automated diagnosis of COVID-19 using X-ray pictures, together with their comparison with our suggested model, is provided in Table 4.

6. CONCLUSION

Medical statistics show that the COVID-19 mortality rate relies on the early and accurate detection of the disease. An appropriate treatment plan with timely intervention through the correct diagnosis of the disease can save many people's lives. Due to many fatalities and the insufficient ability to diagnose critical cases, there is an urgent need for computer-aided diagnosis. This model utilises an updated VGG-16 architecture, which was trained on an X-ray image dataset from two distinct public data sources consisting of 1,320 and 1578 cases in two classes (COVID-19 and normal), respectively. As the paper points out, the model has shown it converges after 50 training epochs. Our approach produced better results without overfitting the data and training in fewer epochs. The overall accuracy, recall, precision, and F1-score all improved with the proposed model when tested on the available dataset, showing that our proposed model achieved an overall accuracy of 99.54%, precision of 100%, recall of 99%, and F1-score of 100%. Medical professionals can use the new method to diagnose people with COVID-19. Additionally, the model is well suited for the examination of different kinds of diseases in the lung using X-ray images after training.

ACKNOWLEDGMENT

This paper has been supported by Duhok Polytechnic University, University of Duhok, and my supervisor. I am grateful for their wonderful assistance in providing me with ongoing advice and assistance throughout my research.

REFERENCES

- [1] Jain, G., Mittal, D., Thakur, D., Mittal, M.K. (2020). A deep learning approach to detect COVID-19 coronavirus with X-Ray images. *Biocybernetics and Biomedical Engineering*, 40(4): 1391-1405. <https://doi.org/10.1016/j.bbe.2020.08.008>
- [2] Abbas, A., Abdelsamea, M.M., Gaber, M.M. (2021). Classification of COVID-19 in chest X-ray images using DeTraC deep convolutional neural network. *Applied Intelligence*, 51(2): 854-864. <https://doi.org/10.1007/s10489-020-01829-7>
- [3] Rahimzadeh, M., Attar, A. (2020). A modified deep convolutional neural network for detecting COVID-19 and pneumonia from chest X-ray images based on the concatenation of Xception and ResNet50V2. *Informatics in Medicine Unlocked*, 19: 100360. <https://doi.org/10.1016/j.imu.2020.100360>
- [4] Karthik, R., Menaka, R., Hariharan, M. (2021). Learning distinctive filters for COVID-19 detection from chest X-ray using shuffled residual CNN. *Applied Soft Computing*, 99: 106744. <https://doi.org/10.1016/j.asoc.2020.106744>
- [5] Al-Timemy, A.H., Khushaba, R.N., Mosa, Z.M., Escudero, J. (2021). An efficient mixture of deep and machine learning models for COVID-19 and tuberculosis detection using x-ray images in resource limited settings. In *Artificial Intelligence for COVID-19*, pp. 77-100. https://doi.org/10.1007/978-3-030-69744-0_6
- [6] El Asnaoui, K., Chawki, Y. (2021). Using X-ray images and deep learning for automated detection of coronavirus disease. *Journal of Biomolecular Structure and Dynamics*, 39(10): 3615-3626. <https://doi.org/10.1080/07391102.2020.1767212>
- [7] Saha, P., Sadi, M.S., Islam, M.M. (2021). EMCNet: Automated COVID-19 diagnosis from X-ray images using convolutional neural network and ensemble of machine learning classifiers. *Informatics in Medicine Unlocked*, 22: 100505. <https://doi.org/10.1016/j.imu.2020.100505>
- [8] Uçar, E., Atila, Ü., Uçar, M., Akyol, K. (2021). Automated detection of COVID-19 disease using deep fused features from chest radiography images. *Biomedical Signal Processing and Control*, 69: 102862. <https://doi.org/10.1016/j.bspc.2021.102862>
- [9] Bohmrah, M.K., Kaur, H. (2021). Classification of COVID-19 patients using efficient fine-tuned deep learning DenseNet model. *Global Transitions Proceedings*, 2(2): 476-483. <https://doi.org/10.1016/j.gltip.2021.08.003>
- [10] Apostolopoulos, I.D., Mpesiana, T.A. (2020). Covid-19: automatic detection from x-ray images utilizing transfer learning with convolutional neural networks. *Physical and Engineering Sciences in Medicine*, 43(2): 635-640. <https://doi.org/10.1007/s13246-020-00865-4>
- [11] Sharifrazi, D., Alizadehsani, R., Roshanzamir, M., et al. (2021). Fusion of convolution neural network, support vector machine and Sobel filter for accurate detection of COVID-19 patients using X-ray images. *Biomedical Signal Processing and Control*, 68: 102622. <https://doi.org/10.1016/j.bspc.2021.102622>
- [12] Ibrahim, D.M., Elshennawy, N.M., Sarhan, A.M. (2021). Deep-chest: Multi-classification deep learning model for diagnosing COVID-19, pneumonia, and lung cancer chest diseases. *Computers in Biology and Medicine*, 132: 104348. <https://doi.org/10.1016/j.compbiomed.2021.104348>
- [13] Panwar, H., Gupta, P.K., Siddiqui, M.K., Morales-Menendez, R., Singh, V. (2020). Application of deep learning for fast detection of COVID-19 in X-rays using nCOVnet. *Chaos, Solitons & Fractals*, 138: 109944. <https://doi.org/10.1016/j.chaos.2020.109944>
- [14] Khan, A.I., Shah, J.L., Bhat, M.M. (2020). CoroNet: A deep neural network for detection and diagnosis of COVID-19 from chest x-ray images. *Computer Methods and Programs in Biomedicine*, 196: 105581. <https://doi.org/10.1016/j.cmpb.2020.105581>
- [15] Bharati, S., Podder, P., Mondal, M.R.H. (2020). Hybrid deep learning for detecting lung diseases from X-ray images. *Informatics in Medicine Unlocked*, 20: 100391. <https://doi.org/10.1016/j.imu.2020.100391>
- [16] Toraman, S., Alakus, T.B., Turkoglu, I. (2020).

- Convolutional capsnet: A novel artificial neural network approach to detect COVID-19 disease from X-ray images using capsule networks. *Chaos, Solitons & Fractals*, 140: 110122. <https://doi.org/10.1016/j.chaos.2020.110122>
- [17] Shibly, K.H., Dey, S.K., Islam, M.T.U., Rahman, M.M. (2020). COVID faster R-CNN: A novel framework to Diagnose Novel Coronavirus Disease (COVID-19) in X-Ray images. *Informatics in Medicine Unlocked*, 20: 100405. <https://doi.org/10.1016/j.imu.2020.100405>
- [18] Abraham, B., Nair, M.S. (2020). Computer-aided detection of COVID-19 from X-ray images using multi-CNN and Bayesnet classifier. *Biocybernetics and Biomedical Engineering*, 40(4): 1436-1445. <https://doi.org/10.1016/j.bbe.2020.08.005>
- [19] Varela-Santos, S., Melin, P. (2021). A new approach for classifying coronavirus COVID-19 based on its manifestation on chest X-rays using texture features and neural networks. *Information Sciences*, 545: 403-414. <https://doi.org/10.1016/j.ins.2020.09.041>
- [20] Heidari, M., Mirniaharikandehi, S., Khuzani, A.Z., Danala, G., Qiu, Y., Zheng, B. (2020). Improving the performance of CNN to predict the likelihood of COVID-19 using chest X-ray images with preprocessing algorithms. *International Journal of Medical Informatics*, 144: 104284. <https://doi.org/10.1016/j.ijmedinf.2020.104284>
- [21] Pandit, M.K., Bandy, S.A., Naaz, R., Chishti, M.A. (2021). Automatic detection of COVID-19 from chest radiographs using deep learning. *Radiography*, 27(2): 483-489. <https://doi.org/10.1016/j.radi.2020.10.018>
- [22] Sheykhivand, S., Mousavi, Z., Mojtahedi, S., Rezaii, T. Y., Farzamia, A., Meshgini, S., Saad, I. (2021). Developing an efficient deep neural network for automatic detection of COVID-19 using chest X-ray images. *Alexandria Engineering Journal*, 60(3): 2885-2903. <https://doi.org/10.1016/j.aej.2021.01.011>
- [23] Adedigba, A.P., Adeshina, S.A., Aina, O.E., Aibinu, A.M. (2021). Optimal hyperparameter selection of deep learning models for COVID-19 chest X-ray classification. *Intelligence-Based Medicine*, 5: 100034. <https://doi.org/10.1016/j.ibmed.2021.100034>
- [24] Hertel, R., Benlamri, R. (2021). COV-SNET: A deep learning model for X-ray-based COVID-19 classification. *Informatics in Medicine Unlocked*, 24: 100620. <https://doi.org/10.1016/j.imu.2021.100620>
- [25] Dilshad, S., Singh, N., Atif, M., et al. (2021). Automated image classification of chest X-rays of COVID-19 using deep transfer learning. *Results in Physics*, 28: 104529. <https://doi.org/10.1016/j.rinp.2021.104529>
- [26] kaggle.com. <https://www.kaggle.com/prashant268/chest-xray-covid19-pneumonia>, accessed on 30 August 2021.
- [27] Curated Chest X-Ray Image Dataset for COVID-19 | Kaggle. <https://www.kaggle.com/unaisait/curated-chest-xray-image-dataset-for-covid19>, accessed on 30 August 2021.
- [28] Thakur, S., Kumar, A. (2021). X-ray and CT-scan-based automated detection and classification of COVID-19 using convolutional neural networks (CNN). *Biomedical Signal Processing and Control*, 69: 102920. <https://doi.org/10.1016/j.bspc.2021.102920>
- [29] Gaur, P., Malaviya, V., Gupta, A., Bhatia, G., Pachori, R. B., Sharma, D. (2022). COVID-19 disease identification from chest CT images using empirical wavelet transformation and transfer learning. *Biomedical Signal Processing and Control*, 71: 103076. <https://doi.org/10.1016/j.bspc.2021.103076>
- [30] Tajbakhsh, N., Shin, J.Y., Gurudu, S. R., Hurst, R.T., Kendall, C.B., Gotway, M.B., Liang, J. (2016). Convolutional neural networks for medical image analysis: Full training or fine tuning? *IEEE Transactions on Medical Imaging*, 35(5): 1299-1312. <https://doi.org/10.1109/TMI.2016.2535302>
- [31] Hahn, S., Choi, H. (2020). Understanding dropout as an optimization trick. *Neurocomputing*, 398: 64-70. <https://doi.org/10.1016/j.neucom.2020.02.067>
- [32] Zhang, W., Du, Y., Yang, Y., Yoshida, T. (2018). DeRec: A data-driven approach to accurate recommendation with deep learning and weighted loss function. *Electronic Commerce Research and Applications*, 31: 12-23. <https://doi.org/10.1016/j.elerap.2021.101064>
- [33] Pezzano, G., Díaz, O., Ripoll, V.R., Radeva, P. (2021). CoLe-CNN+: Context learning-convolutional neural network for COVID-19-Ground-Glass-Opacities detection and segmentation. *Computers in Biology and Medicine*, 136: 104689. <https://doi.org/10.1016/j.compbimed.2021.104689>
- [34] Hassantabar, S., Ahmadi, M., Sharifi, A. (2020). Diagnosis and detection of infected tissue of COVID-19 patients based on lung X-ray image using convolutional neural network approaches. *Chaos, Solitons & Fractals*, 140: 110170. <https://doi.org/10.1016/j.chaos.2020.110170>
- [35] Fang, L., Wang, X. (2021). COVID-19 deep classification network based on convolution and deconvolution local enhancement. *Computers in Biology and Medicine*, 135: 104588. <https://doi.org/10.1016/j.compbimed.2021.104588>

NOMENCLATURE

I_j	Input image
L	Loss function
δ_j	Bernoulli distribution of probability
s_i	Dropout neuron
W_{ij}	Weight of neuron
y_i	Predicted output
\hat{y}_i	Actual output of model